


SEMA7A as a Novel Prognostic Biomarker and Its Correlation with Immune Infiltrates in Breast Cancer

Shiyu Zhang, Fanting Kong, Lei Zheng, Xiaowei Li, Lining Jia, Lixian Yang 

Department of Breast Surgery, Xingtai People's Hospital, Xingtai, Hebei, 054000, People's Republic of China

Correspondence: Lixian Yang, Department of Breast Surgery, Xingtai People's Hospital, No. 818 Xiangdu District, Xingtai, Hebei, 054000, People's Republic of China, Email yanglixian@hebmu.edu.cn

Background: The role of Semaphorin 7a (SEMA7A) in the initiation and progression of different types of cancerous lesions has been extensively studied. However, the prognostic significance of SEMA7A, specifically in breast cancer (BC), lacks clarity.

Methods: We conducted an evaluation on the relationship between SEMA7A and the prognosis, immune invasion and tumor mutation burden in different types of cancer by analyzing data from The Cancer Genome Atlas database. The present study focused on investigating the expression level, mutation, immune correlation and coexpression of SEMA7A in BC, utilizing various databases such as the University of Alabama at Birmingham Cancer data analysis portal, cBioPortal and tumor immune estimation resource. Survival analysis was carried out using the Kaplan-Meier Plotter. Furthermore, we employed the R software package to generate receiver operating characteristic (ROC) curves and nomograms. Notably, $P < 0.05$ was considered to indicate statistical significance.

Results: Using pancancer analysis, it has been observed that the expression of SEMA7A is elevated in various types of cancer and is strongly correlated with the prognosis of different cancer types. SEMA7A also exhibits a significant association with the tumor mutation burden of diverse types of cancer. Moreover, SEMA7A displays a notable increase in BC cases, and was indicated to have a substantial association with the abundance of immune infiltration. In-depth survival analysis demonstrated that elevated levels of SEMA7A expression are notably linked to shorter overall survival and distant metastasis-free survival among patients with BC. The efficiency of SEMA7A as a reliable prognostic biomarker for BC has been substantiated by the validation of ROC curves and nomograms.

Conclusion: SEMA7A has the potential to function as a prognostic indicator for BC, and its correlation with immune infiltration in BC is significant.

Keywords: SEMA7A, breast cancer, biomarker, prognosis, methylation, immune infiltration, nomogram, bioinformatics

Introduction

Breast cancer (BC), also known as BRCA, is a prevalent malignancy affecting women worldwide.¹ It stands as one of the leading causes of cancer-related deaths and has the highest occurrence rate among all cancers in women.^{2,3} Current statistics show that BC accounted for approximately 30% of diagnosed cancer cases in women in the United States in 2021.³ The United States was projected to witness 284,200 newly diagnosed cases of BC in 2021, with an estimated 44,130 deaths resulting from this disease.³ Nevertheless, numerous aspects of the precise molecular biological mechanism underlying the onset and progression of BC remain uncertain. Furthermore, the detection rate for early-stage BC is inadequate, and the therapeutic interventions are associated with significant adverse effects, resulting in subpar outcomes in the clinical management of this malignancy.⁴⁻⁶ The biological heterogeneity of patients with BC hampers the ability of the current staging system to accurately predict their prognosis. Additionally, the characteristics of tumor cells can impact the clinical outcome of patients. Exploiting these features to develop prognostic markers may enhance the current TNM staging system, leading to improved clinical prediction and better treatment planning.⁷

Semaphorin 7a (SEMA7A), also known as CDw108, is a type of membrane glycoprotein that is attached to the cell through a structure called the glycosylphosphatidylinositol (GPI) anchor.⁸ The expression of SEMA7A has been shown to be higher in activated T lymphocytes, erythrocytes and certain leukemia cell lines.⁸ In addition, SEMA7A mRNA expression has been observed in some adult tissues, such as the placenta, testis, lung, brain, thymus and spleen. Roles for SEMA7A have been identified in neuronal guidance and immune modulation.^{9–11} After the cleavage of the GPI membrane anchor, the SEMA7A protein has the ability to exist as either a shed form or a membrane-bound form. Once SEMA7A is shed, it can exert its influence in both cell autonomous and non-autonomous manners. Consequently, SEMA7A has demonstrated its capability to enhance the mobility of melanocytes, neuronal cells and immune cells by activating β -1 integrin signaling.^{9,10,12} In recent years, SEMA7A has been characterized as a tumor promoter. Specifically, SEMA7A fosters the advancement of tumors by promoting the growth of tumors, increasing their invasiveness, facilitating adhesion to extracellular matrices associated with tumors, inducing epithelial to mesenchymal transition, and fostering metastasis in melanoma and glioblastoma, as well as in oral cancer.¹³ These investigations demonstrate the significance of SEMA7A in the initiation and progression of numerous cancerous growths. By performing pancancer research and conducting bioinformatics analysis on SEMA7A in relation to BC, our comprehension of the associated roles of SEMA7A in BC will be improved. This, in turn, will supply novel perspectives for the development of drugs for BC and facilitate the clinical exploration of molecular markers for diagnosing and predicting the prognosis of this disease.

Materials and Methods

Bioinformatics Analysis of RNA-Sequencing (Seq) Data

The breast adenocarcinoma (BRCA) dataset from The Cancer Genome Atlas (TCGA) (<http://tcga.xenahubs.net>) was employed to standardize the RNA-seq information and ascertain the clinical characteristics connected with BRCA mutations. For further examination, a total of 1087 BC and 113 complete breast tissues were retrieved, having three diverse levels of HTSeq fragments.

Collection of Pathological Samples

Between August 2021 and June 2023, we collected a total of 15 BC tissue samples, along with their respective normal tissue samples, from the Breast Surgery Department at Xingtai People's Hospital. The research conducted in this study received approval from the Medical Ethics Committee of Xingtai People's Hospital and adhered to the principles outlined in the Declaration of Helsinki.

Tumor Immune Estimation Resource (TIMER) Database Analysis

The utility of this approach lies in its ability to examine gene expression and the presence of immune cells within tumors across an extensive variety of cancer types by means of a centralized database (TIMER 2.0; <http://cistrome.shinyapps.io/timer/>). In the present investigation employing TIMER, the researchers analyzed the levels of SEMA7A expression in tumors and contrasted them with those observed in normal tissues. They employed TIMER to explore the connection between SEMA7A and the expression levels of immune cells infiltrating tumors, as well as immune cell markers. The link between immune cell infiltration and gene expression in TIMER was assessed through the application of Spearman correlation analysis.

University of Alabama at Birmingham Cancer (UALCAN) Data Analysis Portal

The UALCAN data analysis portal (<http://ualcan.path.uab.edu/index.html>) facilitates the online analysis of gene expression disparities between cancer types and their corresponding normal tissues. This platform utilizes TCGA-RNA-seq datasets and clinical datasets to compare and contrast gene expression patterns among 31 different cancer types. Apart from delivering survival prognostic information, this online tool focuses on identifying variations in gene expression.

cBioPortal

The cBio Cancer Portal (cBioPortal) is a comprehensive web resource which provides multidimensional visualization and access to cancer genomics data (www.cbioportal.org). In the present study, gene mutations of ARFs in BRCA were analyzed using this resource.

GeneMania

GeneMania is a website abundant in gene details, gene list analysis, and gene function analysis prioritized by a high-precision prediction algorithm (<http://www.genemania.org>). To construct the ARF interaction networks, we utilized this resource-rich website.

String

The online database known as STRING (<https://string-db.org/>) facilitates the exploration of protein-protein interactions (PPIs). By analyzing the PPI network in STRING, we can identify and evaluate the diverse expression levels and potential PPIs associated with ARFs.

Nomogram and Calibration Curve Construction

The ‘rms’ and ‘survival’ packages in R were used to construct nomogram models based on SEMA7A expression. The estimation of the concordance between predicted and actual survival was performed by utilizing calibration curves.

Differentially Expressed Gene (DEG) Analysis

Based on the median SEMA7A expression score, breast cancer patients from TCGA were categorized into two groups: High and low SEMA7A expression groups. The DESeq2 R package was utilized to analyze the DEGs between these two groups, with thresholds set at an adjusted P-value of 2.

Functional Enrichment Analysis

The DEGs were subjected to functional enrichment analyses using the R package GOpot (version 1.0.2) to perform Gene Ontology (GO) and Kyoto Encyclopedia of Genes and Genomes (KEGG) analysis.

Analyses of Immune Infiltration

The current investigation aimed to assess the extent of tumor immune infiltration using the single sample gene set enrichment analysis approach implemented in the ‘GSVA’ R package. The datasets obtained from TCGA were utilized for this purpose. To examine the relationship between SEMA7A expression and the infiltration of immune cell types, the analysis involved Spearman’s rank correlation coefficient. For the visualization of data, graphs and figures were generated using the ‘ggplot2’ R package. Additionally, Spearman and Wilcoxon rank sum tests were employed to assess the impact of any observed deviations.

Cultures and Cell Lines

The following human BC cell lines: MCF-7, SKBR-3 and BT549 were purchased from Procell Life Science & Technology Co., Ltd. Additionally, the MCF10A normal breast epithelial cell line was obtained from Procell Life Science & Technology Co., Ltd. The cells were cultured in specific media and supplements. The routine culture for SKBR-3, MCF-7 and BT549 cells involved DMEM (Gibco; Thermo Fisher Scientific, Inc.) with 10% fetal bovine serum (Gibco; Thermo Fisher Scientific, Inc.) and 1% penicillin and streptomycin (Beyotime Institute of Biotechnology). On the other hand, MCF10A cells were maintained in mammary epithelial cell medium (Procell Life Science & Technology Co., Ltd). The medium for MCF10A cells was supplemented with 10% horse serum (Procell Life Science & Technology Co., Ltd), EGF (Procell Life Science & Technology Co., Ltd), hydrocortisone (Procell Life Science & Technology Co., Ltd), insulin (Procell Life Science & Technology Co., Ltd), and 1% penicillin-streptomycin. The cell lines were passaged using standard cell culture techniques in a CO₂ incubator set at 37°C.

Reverse Transcription-Quantitative PCR (RT-qPCR)

A RNAiso Plus Kit (cat. no. 9109; Takara Biotechnology Co., Ltd.) was used to isolate total RNA from SKBR-3, MCF-7, BT549 and MCF10A cells according to the manufacturer's protocol. RT was conducted with the PrimeScript™ RT Reagent Kit and the genomic DNA Eraser; a total of 1000 ng mRNA was converted to cDNA (cat. no. RR047; Takara Bio, Inc.) according to the manufacturer's protocol. A LightCycler® 96 instrument (Roche Diagnostics) was used to perform qPCR analysis using TB Green Premix Ex Taq (cat. no. RR420; Takara Bio, Inc.) to detect the expression levels of the target genes. The following primer pairs were used for qPCR: SEMA7A forward, 5'-TTCAGCCCGGACGAGAACT-3' and reverse, 5'-GAACCGAGGGATCTCCCAT-3'; and GAPDH forward, 5'-GGAGCGAGATCCCTCCAAAAT-3' and reverse, 5'-GGCTGTTGTCATACTTCTCATGG-3'. The thermal cycling conditions for qPCR were as follows: 95°C for 5 min, followed by 40 cycles at 95°C for 10 sec and 60°C for 30 sec. The relative cycle threshold of the endogenous control gene GAPDH was used to normalize the rate of relative mRNA expression levels using the standard $2^{-\Delta\Delta C_q}$ method. Triplicates of each experiment were performed.

Cell Transfection

Lipofectamine® 3000 (Invitrogen; Thermo Fisher Scientific, Inc.) was used to perform transfection with SEMA7A small-interfering (si)RNA and a negative control in MCF7 and BT549 cells. The sequences of siRNA against SEMA7A were: sense sequence: CGCUGCGGCUGCGGCUGCUGCUGCU, antisense sequence: AGCAGCAGCAGCCGAGCCGAGCCGAGCG, and the sequences of negative control were: sense sequence: CGCGCCGGUGCCGGUUCGGUGUGCU, antisense sequence: AGCACACGGAACCGGCACCGGCGCG. Transfections were carried out at a concentration of 100 nM at 37°C for 6 h. Following transfection, the experiments were conducted after 48 h.

Cell Proliferation Assay

To evaluate cell proliferation, the Cell Counting Kit-8 (CCK-8) assay provided by Dojindo Laboratories, Inc. was employed. Briefly, 96-well plates were utilized to plate MCF7 or BT549 cells, at a density of 2×10^3 cells per well. After an initial 24, 48 or 72-h incubation at 37°C, a subsequent incubation was conducted for 4 h at the same temperature. The absorbance of each well at 450 nm was determined using a Multiskan Sky microplate reader from Thermo Fisher Scientific, Inc.

Wound Healing Assay

After transfection, a 35-mm² petri dish was used to incubate 2×10^5 MCF7 or BT549 cells for 48 h at 37°C. To remove detached cells, a 200 µL pipette tip was employed to scratch the monolayer. The cells located in the remaining wound were cultured in media without serum, and the closure of the wound was observed. Images of the wounds were captured at 0 and 24 h after the scratching process using an Olympus light microscope (Olympus Corporation) at a magnification of x100. The wound closure was quantified using ImageJ software version 1.47. Mobility ratio, a measurement of migratory ability, was calculated using the following formula: Mobility ratio = (scratch width at 24 h - scratch width at 0 h) / scratch width at 0 h.

Statistical Analysis

Bioinformatics analysis was carried out using R version 4.2.2 (<http://www.r-project.org/>). Comparisons between or among groups were performed using unpaired Student's *t*-test, paired Student's *t*-test, Mann-Whitney *U*-test or one-way ANOVA. Tukey's HSD was used as a post hoc test following ANOVA. To determine the predictive value of SEMA7A expression for BC diagnosis, receiver operating characteristic (ROC) analysis was conducted between BC tumors and paracancerous tissues. In order to determine the relationship between SEMA7A expression levels and patient survival, the Kaplan-Meier (KM) plotter was used. The TCGA-BRCA dataset was divided into high and low SEMA7A expression groups based on median expression. An R package called "Forest plot" was used to visualize the results of a one-way Cox survival analysis. The statistical analysis of clinical features and SEMA7A expression was conducted using the Mann-Whitney *U*, Wilcoxon signed rank and Fisher's exact tests, as well as logistic regression. Spearman rank correlation test was used for the correlation analysis between SEMA7A and co-expressed genes. Dunnett's post-hoc

test was used to compare the levels of SEMA7A expression between BC and normal breast epithelial cells. Each experiment was repeated three times, and the data are presented as the mean \pm standard deviation. $P < 0.05$ was considered to indicate a statistically significant difference.

Results

Aberrant upregulation of SEMA7A expression in BC. The analysis of the TIMER database included analysis of SEMA7A expression profiles among various cancer types. The analysis indicated that the expression levels of SEMA7A were significantly upregulated in the majority of cancer tissues, including BRCA, cholangiocarcinoma, esophageal carcinoma, head and neck squamous cell carcinoma, liver hepatocellular carcinoma, lung adenocarcinoma, lung squamous cell carcinoma and stomach adenocarcinoma compared with those detected in their corresponding normal tissues (Figure 1A). The analysis of TCGA database included assessment of SEMA7A expression profiles among various cancer types for which paired tissues were available. The analysis indicated that the expression levels of SEMA7A were significantly upregulated in several cancer tissues, including BRCA, cholangiocarcinoma, colon adenocarcinoma, esophageal carcinoma, liver hepatocellular carcinoma, head and neck squamous cell carcinoma and uterine corpus endometrial carcinoma (Figure 1B). A total of 1087 BC and 113 normal breast tissues were collected from TCGA-BRCA dataset to examine the expression levels of SEMA7A in BC and normal tissues in more detail. A significant difference was found between normal and BC tissues with regard to the expression levels of SEMA7A ($P < 0.001$; Figure 1C). The comparison of 112 BC tissues with their matched adjacent normal tissues demonstrated that BC tissues expressed significantly higher levels of SEMA7A than those of normal tissues ($P < 0.001$; Figure 1D). Furthermore, ROC curves were used to determine the area under the curve (AUC) to evaluate the effectiveness of SEMA7A mRNA expression levels in detecting BC. With an AUC of 0.819, SEMA7A could serve as a biomarker for distinguishing BC from non-tumor tissues (Figure 1E). RT-qPCR analysis revealed that 15 BC tissues from Xingtai People's Hospital expressed considerably higher levels of SEMA7A than those of normal breast tissues ($P < 0.001$; Figure 1F). The clinicopathological information of the patients is presented in Table 1. In addition, all three types of BC cells tested expressed significantly higher levels of SEMA7A than those detected in MCF10A cells (Figure 1G).

Association between SEMA7A expression and clinicopathological variables. Based on the information presented in Table 2 and Figure 2, there was a notable correlation between the expression levels of SEMA7A and various factors, such as individual cancer stage, age, subclass, menopause status and nodal metastasis status. Through the use of univariate logistic regression analysis, several clinicopathological distinctions were observed between the groups with high and low SEMA7A expression. These distinctions included age ($P < 0.001$), PAM50 subtype classification ($P < 0.001$), estrogen receptor status ($P < 0.001$), menopause status ($P = 0.041$), and progesterone receptor status ($P < 0.001$), as demonstrated in Table 3.

Expression of SEMA7A and methylation. To examine the link between the expression levels of SEMA7A and the methylation status observed in BC tissues, we utilized online tools. In line with data from the UALCAN database, DNA methylation levels were notably higher in BC tumor tissues compared with in normal breast tissues ($P < 0.001$; Figure 3A). Furthermore, we found a significant correlation between the DNA methylation levels of SEMA7A and various factors, including menopause status ($P < 0.001$; Figure 3B), age ($P < 0.001$; Figure 3C), subclass ($P < 0.001$; Figure 3D), nodal metastasis status ($P < 0.001$; Figure 3E), individual cancer stage ($P < 0.001$; Figure 3F), sex ($P < 0.001$; Figure 3G) and ethnicity ($P < 0.001$, Figure 3H).

Prognostic value of SEMA7A expression in BC. Utilizing the KM technique, we observed a link between the prognostic value of BC and the expression of SEMA7A. In this investigation, we employed SEMA7A expression as a criterion to categorize patients into two distinct groups: High and low. Notably, high SEMA7A expression demonstrated a significantly unfavorable prognosis in terms of distant metastasis-free survival (DMFS; Figure 4B) and overall survival (OS; Figure 4C) when compared with low SEMA7A expression (OS: $P = 0.034$; DMFS: $P = 0.014$). Conversely, no significant correlation was established between SEMA7A and recurrence-free survival in breast cancer (Figure 4A).

Construction and validation of a nomogram and prognostic calibration curve based on independent factors. A nomogram was created for patients with BC, utilizing OS, disease-specific survival and progression-free interval as individual indicators of prognosis. The nomograms demonstrated that a greater total point value was associated with

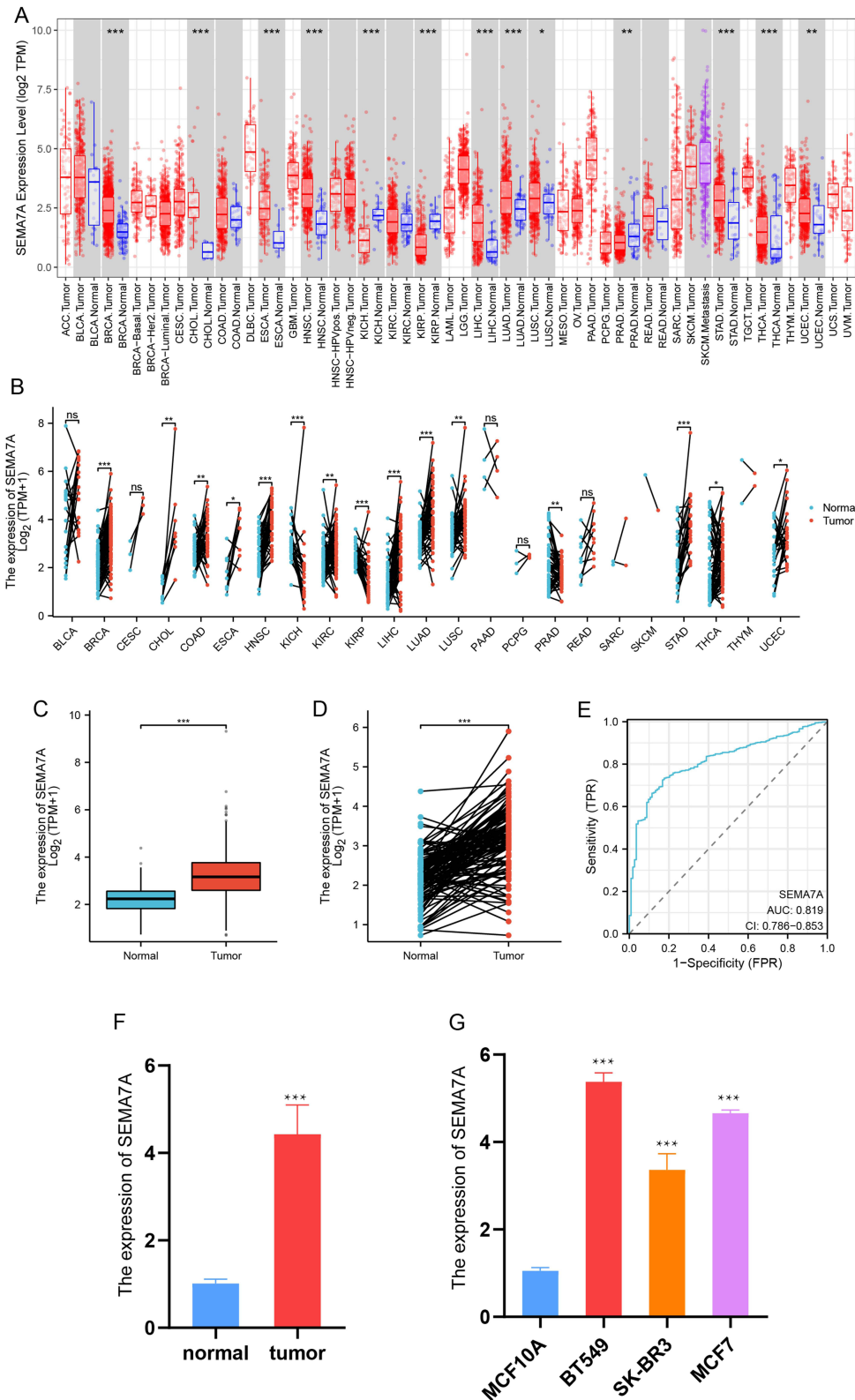


Figure 1 Expression levels of SEMA7A in BRCA. **(A)** Unpaired analysis of SEMA7A expression (mean ± SD) in 33 types of cancer based on bioinformatics data. **(B)** Paired analysis of SEMA7A expression (mean ± SD) in 23 types of cancer based on bioinformatics data. **(C)** Unpaired analysis of SEMA7A expression (mean ± SD) between tumor and normal tissues in 1087 patients with BRCA. **(D)** Paired analysis of SEMA7A expression (scatter points represent expression levels of individual samples) between tumor and normal tissues (n=113). **(E)** A ROC curve was used to establish the efficiency of SEMA7A mRNA expression levels in distinguishing BRCA tumor from non-tumor tissues. The X-axis represents the false positive rate and the Y-axis represents the true positive rate. **(F)** Comparison of SEMA7A mRNA expression levels between normal and tumor tissues from Xingtai People's Hospital. **(G)** Relative expression levels of SEMA7A mRNA in BC cells and a normal breast cell line. Unpaired/paired Student's t-test was used to analyze the data. *P<0.05, **P<0.01, ***P<0.001 vs normal.

Abbreviations: BRCA, breast adenocarcinoma; TCGA, The Cancer Genome Atlas; ROC, receiver operating characteristic; BC, breast cancer; ns, not significant.

Table 1 Clinicopathological Characteristics of Patients with Breast Cancer (n=15) in the Present Study

Characteristics	Patients, n (%)
Age, years	
≤50	5(33.3)
>50	10(66.7)
Tumor size, cm	
≤3	6(40)
>3	9(60)
Grade	
II	4(26.7)
III	11(73.3)
TNM stage	
I	4(26.7)
II	4(26.7)
III	7(46.7)
ER status	
Positive	10(66.7)
Negative	5(33.3)
PR status	
Positive	10(66.7)
Negative	5(33.3)
HER2 status	
Positive	6(40)
Negative	9(60)
Ki-67, %	
≤20	6(40)
>20	9(60)
Lymph node status	
Positive	5(33.3)
Negative	10(66.7)

Table 2 Clinicopathological Characteristics of High- and Low- SEMA7A Expression Groups. The Wilcoxon Rank-Sum Test Was Used to Analyze the Data

Characteristics	Low Expression of SEMA7A	High Expression of SEMA7A	P value
n	543	544	
Pathologic T stage, n (%)			0.619
T1	135 (24.9%)	143 (26.3%)	
T2	311 (57.3%)	320 (58.8%)	
T3	77 (14.2%)	63 (11.6%)	
T4	18 (3.3%)	17 (3.1%)	
unknown	2(0.4%)	1(0.2%)	
Pathologic N stage, n (%)			0.239
N0	250 (46.0%)	266 (48.9%)	
N1	193 (35.5%)	166 (30.5%)	
N2	51 (9.4%)	65 (11.9%)	
N3	38 (7.0%)	39 (7.2%)	
unknown	11(2.0%)	8(1.5%)	

(Continued)

Table 2 (Continued).

Characteristics	Low Expression of SEMA7A	High Expression of SEMA7A	P value
Pathologic M stage, n (%)			0.196
M0	449 (82.7%)	456 (83.8%)	
M1	7 (1.3%)	13 (2.4%)	
unknown	87(16.0%)	75(13.8%)	
Pathologic stage, n (%)			0.763
Stage I	88 (16.2%)	94 (17.3%)	
Stage II	313 (57.6%)	306 (56.3%)	
Stage III	122 (22.5%)	122 (22.4%)	
Stage IV	7 (1.3%)	11 (2.0%)	
unknown	13(2.4%)	11(2.0%)	
Age, n (%)			< 0.001
<= 60	274 (50.5%)	329 (60.5%)	
> 60	269 (49.5%)	215 (39.5%)	
PR status, n (%)			< 0.001
Negative	127 (23.4%)	215 (39.5%)	
Indeterminate	3 (0.5%)	1 (0.2%)	
Positive	380 (70.0%)	312 (57.4%)	
unknown	33(6.1%)	16(2.9%)	
ER status, n (%)			< 0.001
Negative	77 (14.2%)	163 (30.0%)	
Indeterminate	0 (0%)	2 (0.4%)	
Positive	434 (80.0%)	363 (66.7%)	
unknown	32(5.9%)	16(2.9%)	
HER2 status, n (%)			0.862
Negative	261 (48.1%)	299 (55.0%)	
Indeterminate	5 (0.9%)	7 (1.3%)	
Positive	70 (12.3%)	87 (16.0%)	
unknown	207(38.1%)	151(27.7%)	
PAM50, n (%)			< 0.001
Normal	14 (2.6%)	26 (4.8%)	
LumA	326 (60%)	238 (43.8%)	
LumB	116 (21.4%)	90 (16.5%)	
Her2-Positive	35 (6.4%)	47 (8.6%)	
Basal	52 (9.6%)	143 (26.3%)	
OS event, n (%)			0.717
Alive	465 (85.6%)	470 (86.4%)	
Dead	78 (14.4%)	74 (13.6%)	
DSS event, n (%)			0.445
No	493 (90.8%)	489 (90%)	
Yes	39 (7.2%)	46 (8.5%)	
unknown	11(2.0%)	9(1.7%)	
PFI event, n (%)			0.939
No	470 (86.5%)	470 (86.4%)	
Yes	73 (13.4%)	74 (13.6%)	

a less favorable prognosis. Multivariate Cox analysis was employed to assign points from the nomogram chart to each variable. By drawing a vertical line connecting the total point axis with each prognostic axis, the estimated survival rates at 1, 3 and 5 years for patients with BC were calculated, facilitating medical practitioners in their clinical decision-making process (Figure 5).

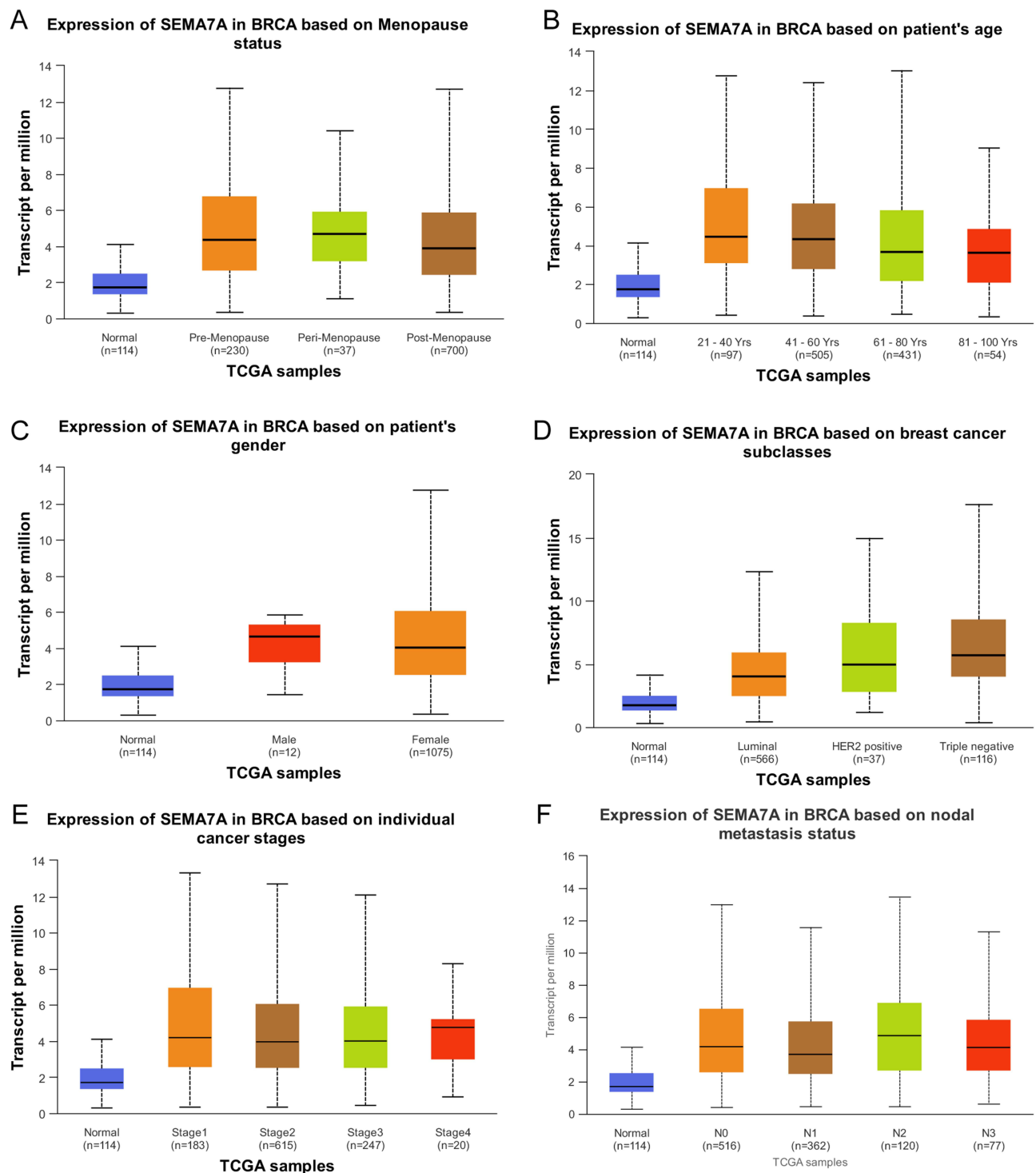


Figure 2 Associations between SEMA7A expression and clinicopathological characteristics. The data are shown for (A) menopause status; (B) age; (C) sex; (D) breast cancer subclass; (E) individual cancer stage; (F) nodal metastasis status. Unpaired Student's t-test was used to analyze the data.

Abbreviations: HER2, human epidermal growth factor receptor 2; UALCAN, University of Alabama at Birmingham Cancer.

Genetic alterations of SEMA7A in breast cancer. Using TCGA dataset, we employed cBioPortal to investigate chromosomal abnormalities and the mutation status of SEMA7A in various cancer types. Our analysis focused on the molecular characteristics of SEMA7A, revealing a mutation rate of 1.7% in BC samples. The most common mutation observed was an amplified mutation, as illustrated in Figure 6A. To establish a protein-protein interaction network, we

Table 3 Associations of SEMA7A Expression with Clinicopathological Characteristics of Patients (n = 1087). Logistic Regression Were Used to Analyze the Data

Characteristics	Total (N)	OR (95% CI)	P value
Pathologic T stage (T3&T4 vs T1&T2)	1084	0.811 (0.586–1.122)	0.206
Pathologic N stage (N2&N3 vs N0&N1)	1068	1.198 (0.877–1.638)	0.257
Pathologic M stage (M1 vs M0)	925	1.829 (0.723–4.626)	0.202
Pathologic stage (Stage III&Stage IV vs Stage I&Stage II)	1063	1.034 (0.782–1.366)	0.816
Age (> 60 vs ≤ 60)	1087	0.666 (0.523–0.847)	< 0.001
PR status (Positive vs Negative)	1034	0.485 (0.372–0.633)	< 0.001
ER status (Positive vs Negative)	1037	0.395 (0.291–0.536)	< 0.001
HER2 status (Positive vs Negative)	717	1.085 (0.760–1.549)	0.654
PAM50 (LumB&LumA vs Her2&Basal)	1047	0.340 (0.254–0.455)	< 0.001
Menopause status (Post vs Pre)	936	0.732 (0.543–0.987)	0.041

Note: The data with statistical significance ($P < 0.05$) were marked in bold text.

utilized the STRING online tool and subsequently identified the hub genes. Figure 6B displays the complex network of DEGs, with the top 10 hub genes being PLXNC1, integrin $\beta 1$ (ITGB1), ITGA1, FYN, SH3GLB2, TAPT1, UNC93B1, SEMA6D, SEMA6B and ABHD8. For a comprehensive understanding of the neighboring genes of SEMA7A, including PLXND1, we utilized Genemania to create gene interaction networks (Figure 6C). These networks highlighted the following neighboring genes: PLXNA3, PLXNC1, NRR2, SEMA3F, PLXNB1, PLXNA4, SEMA3A, KDR and SEMA6A.

Identification of DEGs in BC. A total of 790 genes were differentially expressed between the groups with high and low expression levels of SEMA7A, including 52 upregulated DEGs (15.6%) and 738 downregulated DEGs (84.4%; adjusted P-value < 0.05 , $|\text{Log}_2\text{-FC}| > 2$; Figure 7A). Subsequently, the relationship between the top 20 DEGs (including ADAM19, CHST11, MSC, ITGA5, SPHK1, PLAUR, TRPV2, ARL4C, MMP9, IL411, ZNF396, BCDIN3D, GIN1, PLA2G12A, ERI2, PTGR2, SCAMP1, USP30, MOAP1 and KCTD3) and SEMA7A was assessed (Figure 7B).

Functional enrichment GO and KEGG analyses. According to the GO enrichment analysis, DEGs were enriched in GO terms, such as “keratinization”, “intermediate filament organization”, “receptor ligand activity” and “intermediate filament cytoskeleton organization” (Figure 7C). A KEGG pathway analysis also revealed significant DEG-enriched pathways, including “Maturity onset diabetes of the young”, “Neuroactive ligand-receptor interaction” and “Primary immunodeficiency” (Figure 7D).

Infiltration of the immune system is correlated with the expression of SEMA7A. Figure 8A shows the frequency of immune cell infiltration into tumors with different SEMA7A mutation statuses in different subgroups of BC. A significant negative correlation was found between the expression of SEMA7A and the infiltration of T helper (Th) 17 cells ($r = -0.268$, $P < 0.001$). A significant positive correlation was found between the expression of SEMA7A and the infiltration of Th1 cells ($r = 0.547$, $P < 0.001$), neutrophils ($r = 0.456$, $P < 0.001$), macrophages ($r = 0.451$, $P < 0.001$), dendritic cells (DCs) ($r = 0.428$, $P < 0.001$), activated DCs ($r = 0.397$, $P < 0.001$), B cells ($r = 0.359$, $P < 0.001$), interstitial DCs ($r = 0.357$, $P < 0.001$) and T cells ($r = 0.347$, $P < 0.001$) (Figure 8B).

BC cell proliferation and migration are influenced by SEMA7A expression. In vitro experiments were conducted to gain a deeper understanding of the biological function of SEMA7A in BC. Both BT549 and MCF7 cells exhibited high expression levels of SEMA7A. To identify the most impactful siRNAs, transfected BT549 and MCF7 cells were subjected to RT-qPCR analysis and Western blotting analysis, which demonstrated their effectiveness (Figure 9A–D). To examine the impact of SEMA7A on BC proliferation and migration, CCK-8 and wound healing assays were performed. The transfection with SEMA7A-siRNA significantly inhibited both the proliferative (Figure 9E and F) and migratory capacities (Figure 9G and H) of BC cells.

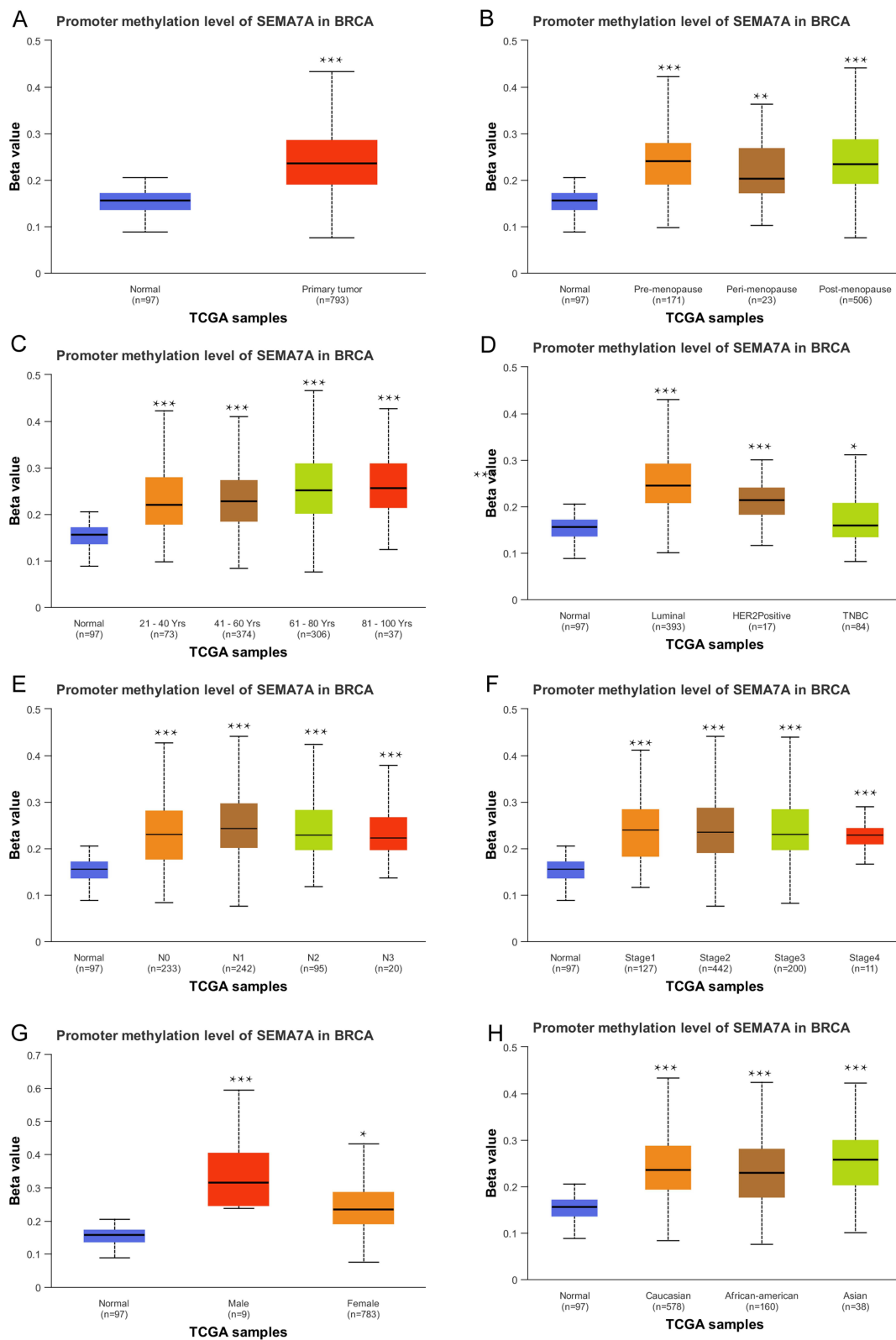


Figure 3 DNA methylation levels of SEMA7A and their effect on the prognosis of patients with BC. Data are shown for (A) sample type; (B) menopause status; (C) age; (D) breast cancer subclass; (E) nodal metastasis status; (F) individual cancer stage; (G) sex, (H) ethnicity.

Abbreviations: BC, breast cancer; UALCAN, University of Alabama at Birmingham Cancer. *P<0.05, **P<0.01 and ***P<0.001.

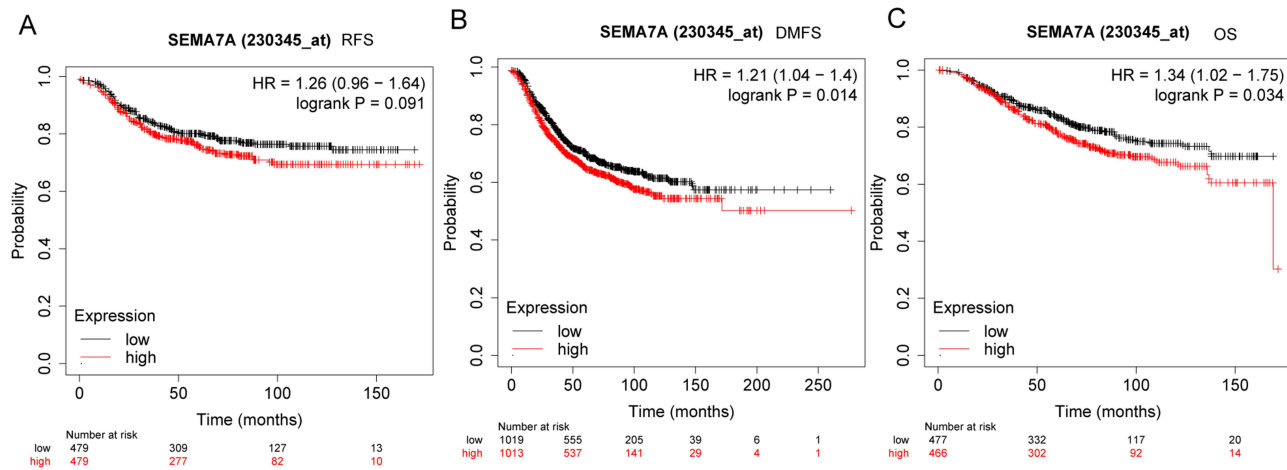


Figure 4 Prognostic values of SEMA7A expression in patients with BC were evaluated by the Kaplan-Meier method. **(A)** RFS, **(B)** DMFS and **(C)** OS of patients with BC with high versus low SEMA7A expression. **Abbreviations:** BC, breast cancer; HR, hazard ratio; OS, overall survival; DMFS, distant metastasis-free survival; RFS, recurrence-free survival.

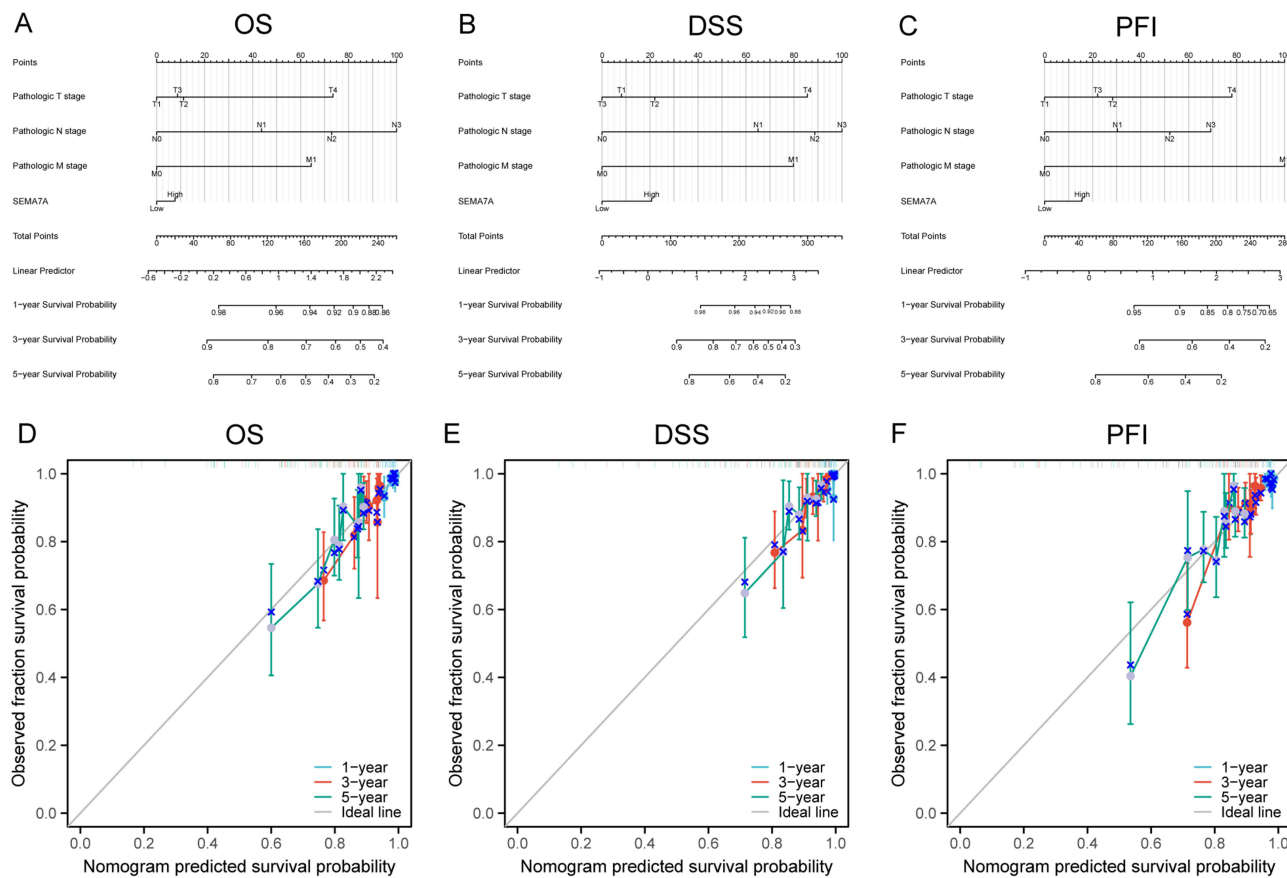


Figure 5 Nomogram for the prediction of 1-, 3- and 5-year **(A)** OS, **(B)** DSS and **(C)** PFI of patients with BC. Calibration curves for the prediction of 1-, 3- and 5-year **(D)** OS, **(E)** DSS and **(F)** PFI of patients with BC. **Abbreviations:** OS, overall survival; DSS, disease-specific survival; PFI, progression-free interval; BC, breast cancer.

Discussion

Semaphorins, a group of secreted or membrane-bound proteins that exhibit high phylogenetic conservation, can be categorized into eight distinct classes according to their sequence similarity and unique structural characteristics.⁹ Initially recognized

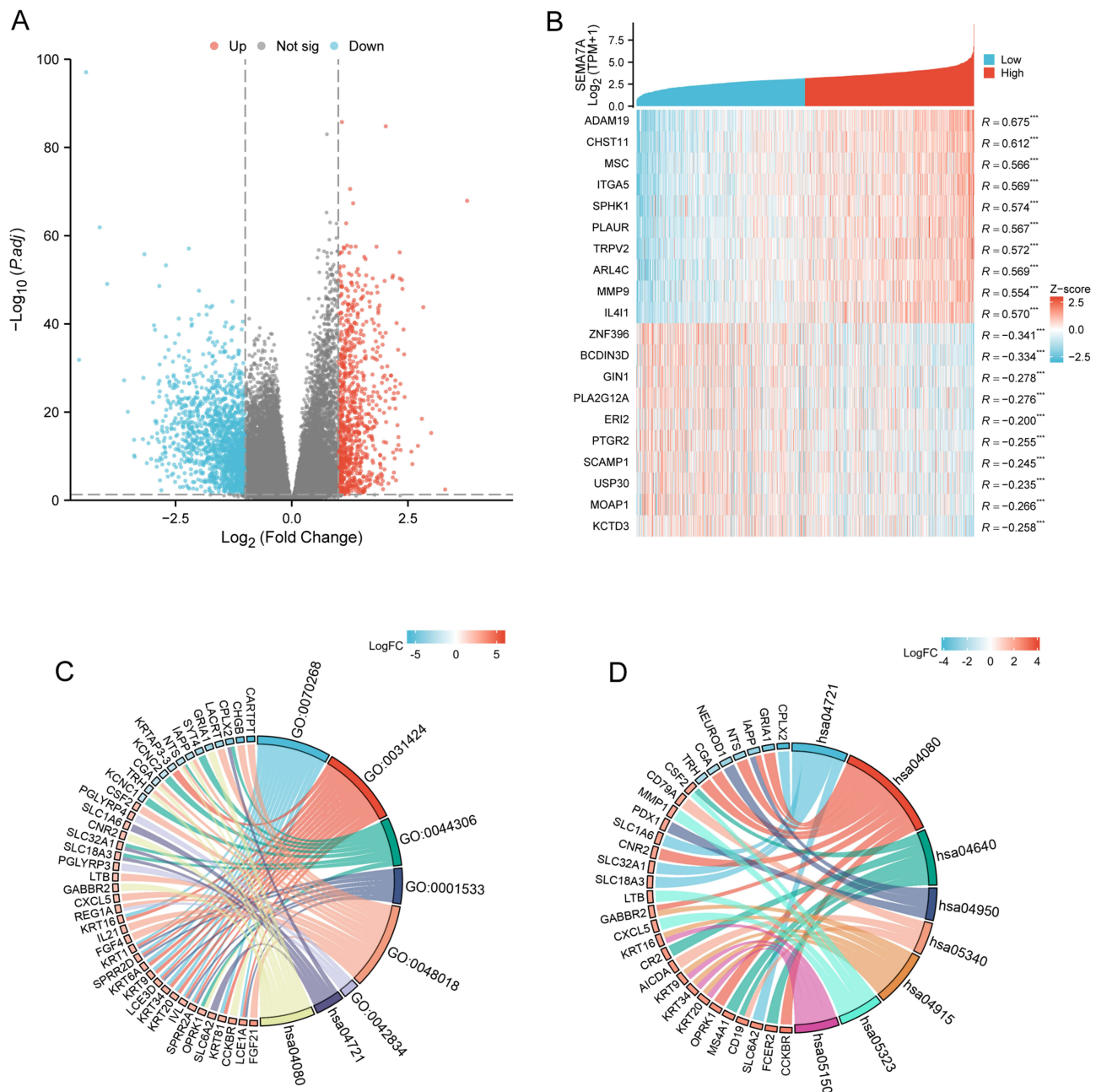


Figure 7 SEMA7A-related DEGs and functional enrichment analysis of SEMA7A in BC using GO and KEGG. **(A)** Volcano plot of DEGs. Blue and red dots indicate the significantly downregulated and upregulated DEGs, respectively. **(B)** Heatmap of the correlation between SEMA7A expression and the top 20 DEGs. **(C)** GO and **(D)** KEGG analysis of DEGs. The correlation between the expression of the top 20 DEGs and SEMA7A was evaluated using Spearman correlation analysis. *** $P < 0.001$. **Abbreviations:** DEGs, differentially expressed genes; BC, breast cancer; GO, Gene Ontology; KEGG, Kyoto Encyclopedia of Genes and Genomes.

anchored protein semaphorin 7A (SEMA7A), which is regulated by mTOR signaling. Analysis of human lung adenocarcinoma specimens revealed a strong association between SEMA7A expression levels and mTOR activation. Through experimentation using cell culture and animal models, it was observed that cells became less resistant to EGFR-TKIs when SEMA7A was lost, while overexpression of SEMA7A increased resistance. These effects on resistance were attributed to the aberrant activation of ERK, resulting in the inhibition of apoptosis. To suppress the ERK signal, knockdown of integrin $\beta 1$ (ITGB1) was performed. Importantly, in patients with EGFR mutant tumors, higher SEMA7A expression levels in clinical samples were indicative of a poorer response to EGFR-TKI treatment. In summary, the SEMA7A-ITGB1 axis plays a critical role in EGFR-TKI resistance by modulating ERK activation and apoptosis

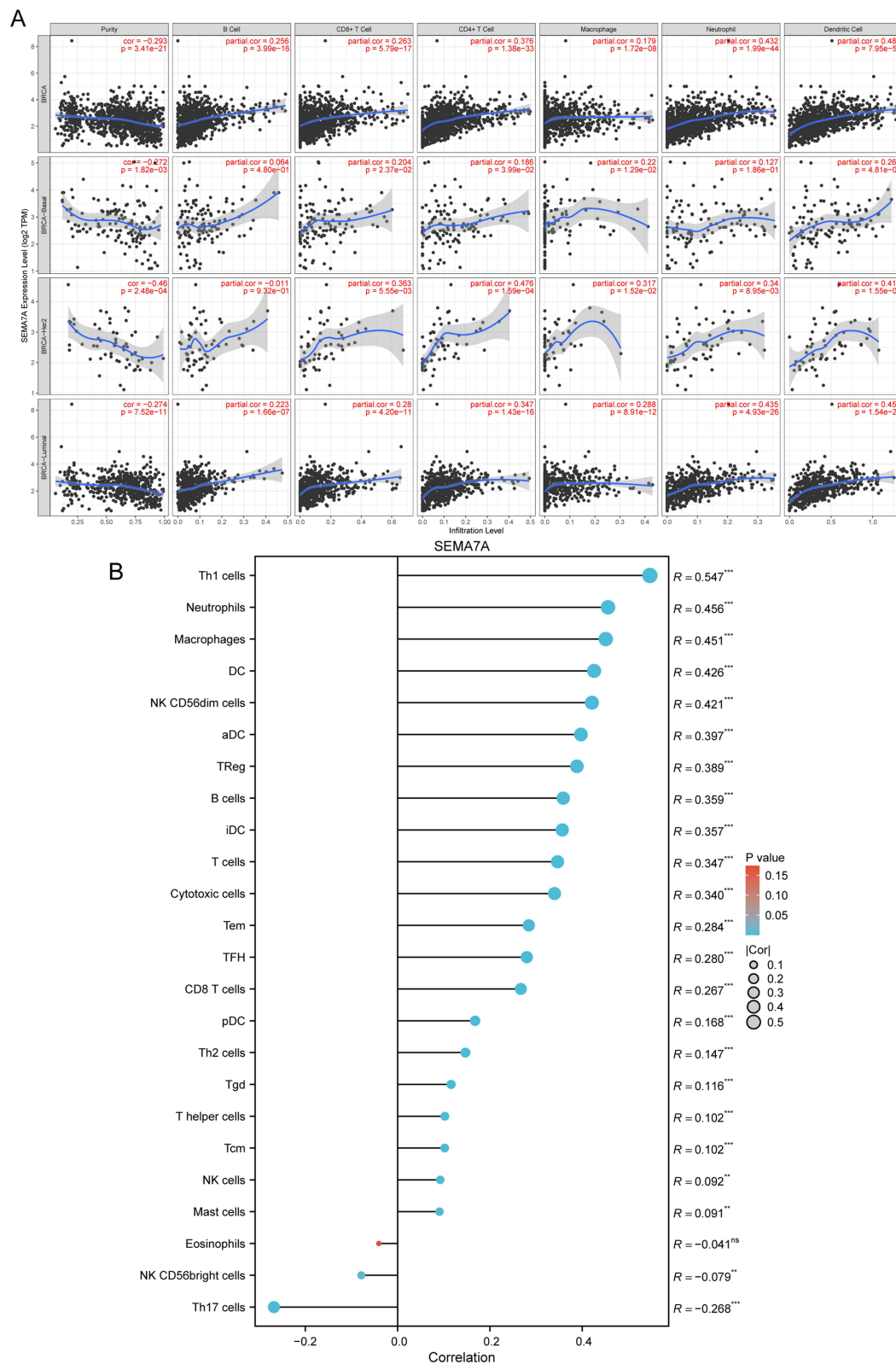


Figure 8 Correlation of SEMA7A expression with immune infiltration levels in BC. **(A)** Correlations between the relative enrichment scores of immune cells and the expression of SEMA7A. **(B)** Correlation between SEMA7A expression and the relative abundance of 24 types of immune cells. The size of the dots corresponds to the absolute Spearman correlation coefficient values. Unpaired Student's t-test was used to analyze the data. The correlation between the expression of SEMA7A and these immune cells was investigated using the Spearman correlation analysis. **P<0.01, ***P<0.005.

Abbreviations: ns, no significance. BC, breast cancer; NK cells, natural killer cells; CD, cluster of differentiation; iDCs, interstitial dendritic cells; TEM cells, effector T cells; pDCs, plasmacytoid dendritic cells.

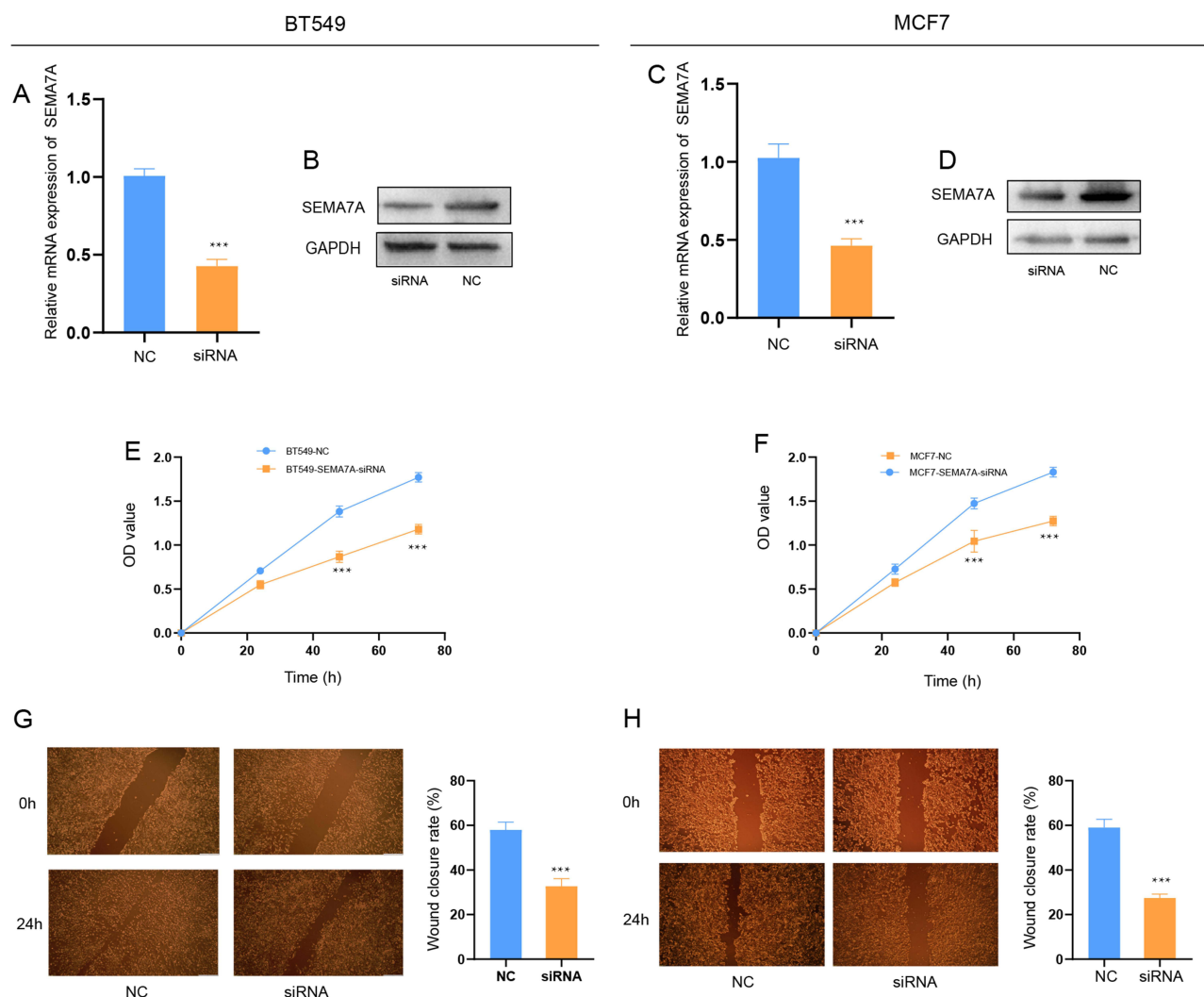


Figure 9 Downregulation of SEMA7A inhibits cell proliferation and migration of breast cancer cells. RT-qPCR analysis of SEMA7A expression levels in (A) BT549 and (C) MCF7 cells transfected with SEMA7A-siRNA and NC. Cell proliferation in (B) BT549 and (D) MCF7 cells transfected with SEMA7A-siRNA and NC. Cell proliferation in BT549 (E) and MCF7 (F) cells transfected with SEMA7A-siRNA and NC. Wound healing assays for (G) BT549 and (H) MCF7 cells transfected with SEMA7A-siRNA and NC. Mann-Whitney *U*-test or one-way ANOVA and unpaired Student's *t*-test was used to analyze the data. ****P* < 0.001.

Abbreviations: RT-qPCR, reverse transcription-quantitative PCR; NC, negative control; siRNA, small interfering RNA; OD optical density.

inhibition. In BC, tyrosine kinase inhibitors are also very important therapeutic tools, and whether SEMA7A plays the same role in BC needs to be confirmed by further experiments. Additionally, increased expression of SEMA7A was associated with a short OS and DMFS of BRCA patients.

DNA methylation is a common epigenetic mechanism that usually leads to the silencing of gene expression.²³ In our investigation of the overexpression of SEMA7A in BRCA, we found indications that it may be associated with DNA hypomethylation of SEMA7A. Tumors often show aberrant DNA methylation, which contributes to their development and progression by either silencing or activating oncogenes. Therefore, we conducted an analysis of the methylation level of SEMA7A in BC tissues, aiming to uncover its potential role in promoting breast carcinogenesis and development. Hopefully, our findings will provide valuable insight into this subject.

The current investigation additionally analyzed the association between the expression of SEMA7A and infiltration of various immune cells. The infiltration of immune cells is a significant contributor to the efficacy of immunotherapy and the prognosis of individuals.^{24–26} Numerous investigations have demonstrated that lymphocytes that infiltrate tumors influence the clinical results of immunotherapy in patients with melanoma, colorectal cancer and ovarian cancer.^{27,28} Garcia-Areas *R et al* found that SEMA7A expression was in an upregulated state in mouse macrophages,²⁹ which is

consistent with our findings in the current study. Their study demonstrates that the expression of SEMA7A is significantly higher in DA-3 murine mammary tumor cells compared to normal mammary cells (Eph4). Additionally, they found that peritoneal elicited macrophages derived from mammary tumor bearing mice exhibit elevated levels of SEMA7A expression when compared to those obtained from normal mice. According to the findings of this investigation, a positive correlation was observed between the levels of SEMA7A and the count of Th1 cells, macrophages and neutrophils. Conversely, it was observed that there exists an inverse relationship between the amount of Th17 cells and NK CD56bright cells and the levels of SEMA7A. Consequently, the presence of SEMA7A often contributes to a bleak prognosis for patients with BC, and the levels of SEMA7A mRNA might serve as an indicator of lymphocyte infiltration. The accurate identification of patient subpopulations in precision medicine heavily relies on the utilization of immunological biomarkers. There are a multitude of immunological biomarkers available, including those related to immune checkpoint inhibitors and tumor mutation burden.

Pathway enrichment analysis of SEMA7A revealed a possible association with “keratinization”, “intermediate filament organization”, “receptor ligand activity” and “intermediate filament cytoskeleton organization”, which may also suggest a possible mechanism for the high expression of SEMA7A in BC tissues and its subsequent association with poor disease prognosis; however, this requires confirmation by more in-depth studies.

To confirm the role of SEMA7A as a prognostic marker in BC, we analyzed clinical samples from patients with this disease. It is important to note that database updates can impact the relationship between SEMA7A and disease prognosis. Additionally, the relationship between SEMA7A mRNA levels and immune cell types and markers may vary as new data become available. As more resources are accumulated, the stratification of data improves, leading to more reliable results. The findings of this study heavily rely on data from public databases. However, it is important to note that these results need to be validated through larger sample sizes and more rigorous experiments. In addition, after analysis, although our siRNA sequence has 100% fitness with SEMA7A, it is possible that there is a certain match with another gene (TACSTD2 or ZYG11B), so we will further verify this in the next study.

The prognostic significance of SEMA7A in BC has been investigated by researchers in the present study. Enhanced expression levels of SEMA7A are commonly observed in BC tissues. In addition, SEMA7A plays a role in immune infiltration and survival. Taken together, these findings propose that SEMA7A holds potential as a biomarker for BC and may be capable of predicting disease prognosis.

Data Sharing Statement

The data generated in the present study are not publicly available due to restrictions applied by Xingtai People’s Hospital but are available from the corresponding author on reasonable request.

Ethics Approval and Consent to Participate

All procedures performed in the present study involving human participants were in accordance with The Declaration of Helsinki (as revised in 2013). The study was approved by the Institutional Ethics Committee of Xingtai People’s Hospital (approval no. 2021[039]). Written informed consent was obtained from each patient.

Author Contributions

All authors made a significant contribution to the work reported, whether that is in the conception, study design, execution, acquisition of data, analysis and interpretation, or in all these areas; took part in drafting, revising or critically reviewing the article; gave final approval of the version to be published; have agreed on the journal to which the article has been submitted; and agree to be accountable for all aspects of the work.

Funding

This study was funded by Xingtai City Key Research and Development Plan (grant no. 2021ZC148) and the Scientific Research Fund of Health Commission of Hebei Province (grant no. 20220224).

Disclosure

The authors declare that they have no competing interests.

References

1. Liang Y, Zhang H, Song X, Yang Q. Metastatic heterogeneity of breast cancer: molecular mechanism and potential therapeutic targets. *In Seminars in Cancer Biol.* 2020;60:14–27. doi:10.1016/j.semcancer.2019.08.012
2. Hong W, Dong EJCL. The past, present and future of breast cancer research in China. *Cancer Lett.* 2014;351(1):1–5. doi:10.1016/j.canlet.2014.04.007
3. Siegel RL, Schulze L, Herbst L, Holzinger R, Klinglmayr T. Geschlechterrepräsentationen in Nachrichtenmedien: ein Werkstattbericht zum Global Media Monitoring Project 2020. kommunikation. *Cancer Stat.* 2021;2021(71):1.
4. Jiralerspong S, Goodwin PJJOCO. Obesity and breast cancer prognosis: evidence, Challenges, and Opportunities. *J Clin Oncol.* 2016;34(35):4203–4216. doi:10.1200/JCO.2016.68.4480
5. Yi-Sheng S, Zhao Z, Yang Z-N, et al. Risk factors and preventions of breast cancer. *Int J Bio Sci.* 2017;13(11):1387–1397. doi:10.7150/ijbs.21635
6. Brook N, Brook E, Dharmarajan A, et al. Breast cancer bone metastases: pathogenesis and therapeutic targets. *Int J Biochem Cell Biol.* 2018;96:63–78. doi:10.1016/j.biocel.2018.01.003
7. Poortmans P, Marsiglia H, De Las Heras M, et al. Clinical and technological transition in breast cancer. *Rep Pract Oncol Radiother.* 2013;18(6):345–352. doi:10.1016/j.rpor.2013.08.002
8. Yamada A, Kubo K, Takeshita T, et al. Molecular cloning of a glycosylphosphatidylinositol-anchored molecule CDw108. *J Immunol.* 1999;162(7):4094–4100. doi:10.4049/jimmunol.162.7.4094
9. Pasterkamp RJ, Peschon JJ, Spriggs MK, et al. Semaphorin 7A promotes axon outgrowth through integrins and MAPKs. *Nature.* 2003;424(6947):398–405. doi:10.1038/nature01790
10. Suzuki K, Okuno T, Yamamoto M, et al. Semaphorin 7A initiates T-cell-mediated inflammatory responses through alpha1beta1 integrin. *Nature.* 2007;446(7136):680–684. doi:10.1038/nature05652
11. Reikoff RA, Peng H, Murray LA, et al. Semaphorin 7a + regulatory T Cells Are Associated With Progressive Idiopathic Pulmonary Fibrosis And Are Implicated In Transforming Growth Factor- β 1-induced pulmonary fibrosis. *Am J Respir Crit Care Med.* 2013;187(2):180–188. doi:10.1164/rccm.201206-1109OC
12. Scott GA, McClelland LA, Fricke AF. Semaphorin 7a promotes spreading and dendricity in human melanocytes through beta1-integrins. *J Invest Dermatol.* 2008;128(1):151–161. doi:10.1038/sj.jid.5700974
13. Ma B, Herzog EL, Lee CG, et al. Role of chitinase 3-like-1 and semaphorin 7a in pulmonary melanoma metastasis. *Cancer Res.* 2015;75(3):487–496. doi:10.1158/0008-5472.CAN-13-3339
14. Czopik AK, Bynoe MS, Palm N, et al. Semaphorin 7A is a negative regulator of T cell responses. *Immunity.* 2006;24(5):591–600. doi:10.1016/j.immuni.2006.03.013
15. Suzuki K, Kumanogoh A, Kikutani H. Semaphorins and their receptors in immune cell interactions. *Nat Immunol.* 2008;9(1):17–23. doi:10.1038/ni1553
16. Kang S, Okuno T, Takegahara N, et al. Intestinal epithelial cell-derived semaphorin 7A negatively regulates development of colitis via α v β 1 integrin. *J Immunol.* 2012;188(3):1108–1116. doi:10.4049/jimmunol.1102084
17. Saito T, Kasamatsu A, Ogawara K, et al. Semaphorin7A promotion of tumoral growth and metastasis in human oral cancer by regulation of G1 cell cycle and matrix metalloproteases: possible contribution to tumoral angiogenesis. *PLoS One.* 2015;10(9):e0137923. doi:10.1371/journal.pone.0137923
18. Formolo CA, Williams R, Gordish-Dressman H, et al. Secretome signature of invasive glioblastoma multiforme. *J Proteome Res.* 2011;10(7):3149–3159. doi:10.1021/pr200210w
19. Lazova R, Gould Rothberg BE, Rimm D, et al. The semaphorin 7A receptor Plexin C1 is lost during melanoma metastasis. *Am J Dermatopathol.* 2009;31(2):177–181. doi:10.1097/DAD.0b013e318196672d
20. Scott GA, McClelland LA, Fricke AF, et al. Plexin C1, a receptor for semaphorin 7a, inactivates cofilin and is a potential tumor suppressor for melanoma progression. *J Invest Dermatol.* 2009;129(4):954–963. doi:10.1038/jid.2008.329
21. Black SA, Nelson AC, Gurule NJ, et al. Semaphorin 7a exerts pleiotropic effects to promote breast tumor progression. *Oncogene.* 2016;35(39):5170–5178. doi:10.1038/onc.2016.49
22. Kinehara Y, Nagatomo I, Koyama S, et al. Semaphorin 7A promotes EGFR-TKI resistance in EGFR mutant lung adenocarcinoma cells. *JCI Insight.* 2018;3(24). doi:10.1172/jci.insight.123093.
23. Lim DH, Maher ER. DNA methylation: a form of epigenetic control of gene expression. *Obstet Gynaecol.* 2010;12(1):37–42. doi:10.1576/toag.12.1.037.27556
24. Stanto SE, Disis MLJFIOC. Clinical significance of tumor-infiltrating lymphocytes in breast cancer. *Journal for Immunotherapy of Cancer.* 2016;4(1). doi:10.1186/s40425-016-0165-6
25. Mahmoud SMA, Paish EC, Powe DG, et al. Tumor-infiltrating CD8 + lymphocytes predict clinical outcome in breast cancer. *J clin oncol.* 2011;29(15):1949–1955. doi:10.1200/JCO.2010.30.5037
26. Miyazaki N, Furuyama T, Sakai T, et al. Developmental localization of semaphorin H messenger RNA acting as a collapsing factor on sensory axons in the mouse brain. *Neuroscience.* 1999;93(1):401–408. doi:10.1016/S0306-4522(99)00134-7
27. Lin B, Du L, Li H, et al. Tumor-infiltrating lymphocytes: warriors fight against tumors powerfully. *Biomed Pharmacother.* 2020;132:110873. doi:10.1016/j.biopha.2020.110873
28. Edwards J, Wilmott JS, Madore J, et al. CD103(+) tumor-resident CD8(+) T cells are associated with improved survival in immunotherapy-naïve melanoma patients and expand significantly during anti-PD-1 treatment. *Clin Cancer Res.* 2018;24(13):3036–3045. doi:10.1158/1078-0432.CCR-17-2257
29. Garcia-Areas R, Libreros S, Amat S, et al. Semaphorin7A promotes tumor growth and exerts a pro-angiogenic effect in macrophages of mammary tumor-bearing mice. *Front Physiol.* 2014;5:17. doi:10.3389/fphys.2014.00017

International Journal of General Medicine

Dovepress

Publish your work in this journal

The International Journal of General Medicine is an international, peer-reviewed open-access journal that focuses on general and internal medicine, pathogenesis, epidemiology, diagnosis, monitoring and treatment protocols. The journal is characterized by the rapid reporting of reviews, original research and clinical studies across all disease areas. The manuscript management system is completely online and includes a very quick and fair peer-review system, which is all easy to use. Visit <http://www.dovepress.com/testimonials.php> to read real quotes from published authors.

Submit your manuscript here: <https://www.dovepress.com/international-journal-of-general-medicine-journal>